PHYSICAL REVIEW B VOLUME 49, NUMBER 23 15 JUNE 1994-I

Pressure dependence of the conductivity and magnetoconductance in oriented iodine-doped polyacetylene

Reghu M., K. Väkiparta,* Y. Cao,[†] and D. Moses
Institute for Polymers and Organic Solids, University of California at Santa Barbara, Santa Barbara, California 93106

(Received 23 July 1993; revised manuscript received 13 January 1994)

The temperature dependences of conductivity and magnetoconductance (MC) have been measured, both parallel and perpendicular to the chain axis, in oriented polyacetylene films doped with iodine. The evolution of anisotropy in conductivity as a function of doping time has been studied. Hydrostatic pressure increases the conductivity for pressures up to 4 kbar; at higher pressure the conductivity gradually decreases. The reduced activation-energy function $[W=-T[d(\ln\rho)/dT]$ is temperature independent in the intermediate temperature region ($T\approx 180-60$ K) suggesting that the material is just on the metallic side of the critical regime of the disorder-induced metal-insulator transition. However, at 8 kbar, $W(T)$ exhibits a positive temperature coefficient from 180 to 1.2 K, implying that the system is more metallic due to enhanced interchain transport. The $T^{1/2}$ dependence of conductivity and the enhanced negative MC, at very low temperatures, indicates that the role of electron-electron interactions is significant. MC measurements have been carried out in all the five different combinations of current with respect to the chain axis and field directions. The sign of MC is positive (negative) when the field is perpendicular (parallel) to the chain axis. The anisotropy in MC is attributed to the anisotropic diffusion coefficient. This is shown by the enhanced positive contribution to the MC at 8 kbar, when the field (current) is parallel (parallel) to the chain axis. At 1.2 K, when both the magnetic field and current are perpendicular to the chain axis, the field-induced crossover from positive to negative MC shows the subtle interplay of weak localization and electron-electron interaction contributions to MC. The inelastic scattering lengths, at 1.2 K, in parallel and perpendicular directions to the chain axis are found to be 1163 and 210 Å, respectively. The $T^{-3/4}$ dependence of the inelastic scattering length at low temperatures is consistent with the $T^{3/4}$ dependence of conductivity. This indicates that the inelastic electron-electron scattering known to be of importance in disordered metals is the dominant scattering mechanism in iodine-doped oriented polyacetylene.

I. INTRODUCTION

The recent paper regarding the logarithmic temperature dependence of resistivity in oriented polyacetylene $(CH)_x$, doped with iodine, has renewed the effort to understand the transport properties in heavily doped "metallic" conducting polymers.[1] The contributions of weak localization and electron-electron interactions to magnetoconductance (MC) provide a guideline for understanding the scattering mechanisms and the quantitative estimation of microscopic transport parameters, e.g., the inelastic scattering length, etc.[2,3] The importance of the roles of localization and interaction in the transport properties of polyacetylene prepared by the Shirakawa route (density ≈ 0.5–0.6 g/cm^3) has been studied in detail by Thummes *et al.*[4] Although resistivities as low as 10^{-5} Ω cm, parallel to the draw direction (chain axis), have been reported for oriented iodine-doped polyacetylene, the positive temperature coefficient for resistivity, typical of a metal, has not been observed.[1] This shows that the limiting factor for the typical metallic temperature dependence of resistivity is the transport perpendicular to the chain axis, which has not been considered in as much detail as the transport parallel to the chain axis in previous studies.[5,6] Thus a comprehensive study of transport has been undertaken in directions both parallel and perpendicular to the chain axis. Magnetoconductance measurements have ben performed in all five different combinations of current with respect to the chain axis and magnetic field.

From the previous transport measurements on iodine-doped oriented $(CH)_x$, it is known that the temperature dependence of both the resistivity and MC depends on the extent of disorder present in the material.[5] For iodine-doped oriented $(CH)_x$ samples having a room-temperature resistivity of 10^{-5} Ω cm, the resistivity ratio[1], $\rho_r=[\rho(1.2\text{ K})/\rho(260\text{ K})]\approx 3$. The magnitude of ρ_r and the sign and magnitude of the MC depend on the extent of disorder.[5] Even though disorder in the pristine material can be reduced considerably by tensile drawing and thereby orienting the $(CH)_x$ chains, the doping process introduces disorder.[7,8] Apart from the variation of the extent of disorder from sample to sample, the degree of anisotropy in oriented $(CH)_x$ plays a significant role in the transport properties, especially in the MC. In previous studies, the maximum draw ratio l/l_0 (l is final length and l_0 is initial length) of the oriented samples was limited to $l/l_0\approx 5-10$.[5,6] Since the samples in the present work were stretch oriented to 15 times, the anisotropic features in the conductivity and MC measurements are rather prominent.

In the present work, we have carried out an extensive study of the electrical conductivity as a function of doping time, pressure, temperature, and magnetic field, in directions both parallel and perpendicular to the chain axis. The maximum room-temperature conductivity in the parallel direction to the chain axis ($\sigma_{\parallel}$) was 2.3×10^4 S/cm. Although this value of conductivity is lower by a factor of 4 compared to that reported in Ref. 1, the values of ρ_r are identical in both samples, which indicates that the extent of disorder in the samples used in the present work and in the samples studied in Ref. 1 are similar. The anisotropy of the conductivity ($\sigma_{\parallel}/\sigma_{\perp}$) at room temperature in directions parallel and perpendicular to the chain axis is $\sigma_{\parallel}/\sigma_{\perp}\approx100$. Hydrostatic pressure increases the conductivity, by a factor of 1.4, up to 4 kbar, and at higher pressures the conductivity gradually decreases. At 8 kbar, the anisotropy in the conductivity has decreased from 105 to 67, indicative of the enhanced interfibrilar and interchain interactions. The temperature dependences of the conductivity, for directions both parallel and perpendicular to the chain axis, are nearly identical. The anisotropic features in the MC are interpreted in terms of anisotropic diffusion coefficient, electron-electron interactions, and weak localization.

The combination of disorder and anisotropy can lead to a wide range of behavior in the transport properties. This is especially true in disordered anisotropic metals, where the importance of electron-electron interactions and disorder-induced localization near the metal-insulator transition (MIT) are well known.[9,10] As will be demonstrated, the field-induced crossover from positive to negative MC shows the subtle interplay of weak-localization and electron-electron-interaction contributions to the MC. From the MC data we derive the inelastic scattering length as a function of temperature, and find that inelastic electron-electron scattering in disordered metals dominates the transport at low temperatures.

II. EXPERIMENTAL DETAILS

Oriented $(CH)_x$ films (density of 1.1 g/cm^3) were prepared according to the nonsolvent method described by Akagi *et al.*[11] and Cao, Smith, and Heeger.[12] The samples were uniaxially stretched by tensile drawing to 15 times the original length, ($l/l_0=15$). The thickness and width of the stretched samples were 8–15 μm and 3–5 mm, respectively. The samples were doped to maximum conductivity by using both iodine vapor and 5-mM solution of iodine in hexane. *In situ* conductivity measurements were carried out while doping.

The dc-conductivity measurements were carried out using both collinear four-probe geometry and the Montgomery method.[13] Samples cut parallel and perpendicular to the chain axis were used for the collinear four-probe measurements, and rectangular samples were used for the Montgomery measurements. Electrical contacts to the samples were made by conductive carbon paint. High-pressure conductivity measurements were carried out in a self-clamped beryllium-copper pressure cell.[14,15] After pressurizing, the cell was clamped at room temperature and then cooled down to 1.2 K in a cryostat containing a superconducting magnet (0–10 T). The hydrostatic pressure-transmitting medium was either fluorinert or a concentrated solution of iodine in fluorinert. All transport measurements used a computer-controlled measuring system; temperature was measured with a calibrated platinum resistor (300–40 K) and a calibrated carbon-glass resistor (40–1.2 K). The power dissipated into the samples was less than 1 μW at low temperatures.

III. RESULTS AND DISCUSSION

A. Time and pressure dependence of the conductivity

In situ conductivity measurements were carried out during both vapor- and solution-phase doping. For solution-phase doping, the sample was immersed in a 5-mM solution of iodine in hexane. The evolution of the conductivity, parallel to the chain axis, as a function of doping time is shown in Fig. 1. The times required to attain the maximum conductivity in vapor (pressure of 1 atm at room temperature) and solution-phase doping are approximately 3 and 8 h, respectively. Maximum conductivities parallel to the chain axis (from vapor and solution phase doping) were 23 000 and 10 000 S/cm, respectively. Thus the kinetics of vapor- and solution-phase doping are not identical. In the direction perpendicular to the chain axis, the maximum conductivity was nearly 200 S/cm (vapor-phase doping). In vapor-phase doping, the conductivity drops after reaching a maximum upon continued exposure to the dopant. The inset in Fig. 1 shows the anisotropy of the conductivity as a function of doping time during solution-phase doping (using the Montgomery method). The maximum value of anisotropy is nearly 110 after 8 h of doping. Although the maximum conductivity (parallel to the chain axis) in vapor-phase doping is 23 000 S/cm, the value of the conductivi-

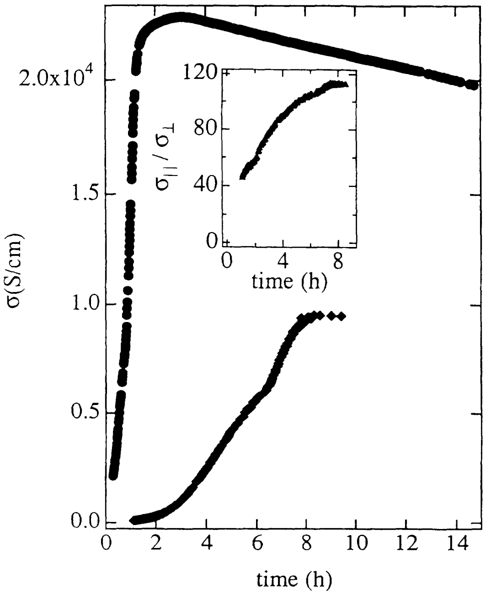

FIG. 1. Conductivity parallel to the chain axis vs doping time for iodine doped $(CH)_x$ in the direction parallel to the chain axis: (●) vapor phase doping, (◆) solution phase doping. The inset shows the anisotropy in the conductivity as a function of doping time.

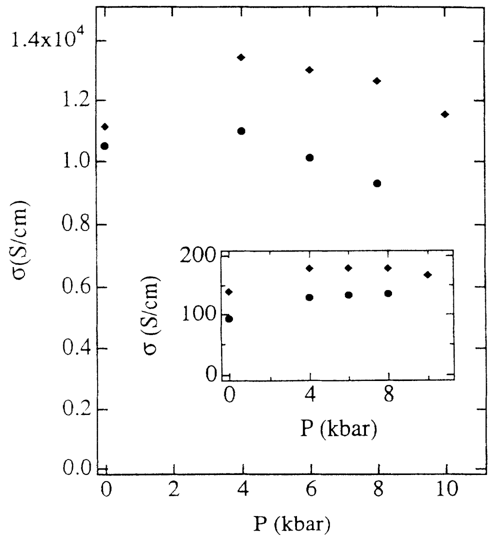

FIG. 2. Conductivity parallel (inset shows conductivity perpendicular) to the chain axis vs pressure for iodine doped $(CH)_x$: (●) samples cut parallel (inset perpendicular) to the chain axis for colinear four-probe technique; and (◆) rectangular samples for Montgomery technique.

ty drops rather rapidly when the sample is removed from the doping cell. Typically, by the time (≈ 30 min) the sample was loaded into the pressure cell or cryostat, the conductivity had reduced to 10 000–12 000 S/cm. This rapid decrease in conductivity is due to the loss of iodine from the sample.

As shown in Fig. 2, the conductivity increases for pressures up to 4 kbar, while at higher pressures the conductivity gradually decreases. The increase in conductivity up to 4 kbar is reversible with pressure, whereas at higher pressures it is not fully reversible. Similar pressure dependence has been observed in previous studies.[16,17] The pressure dependence of conductivity in potassium-doped orientated $(CH)_x$ is also nearly identical.[18] The inset in Fig. 2 shows the pressure dependence of the conductivity in the direction perpendicular to the chain axis. The initial increase is attributed to enhanced interchain transport, while the decrease above 4 kbar is not understood. At 8 kbar, the anisotropy ($\sigma_\parallel/\sigma_\perp$) has reduced by a factor of 1.6, from 110 to 67, at room temperature. The pressure dependence of the conductivity is identical in directions both parallel and perpendicular to the chain axis, implying that the macroscopic conductivity in both directions is apparently governed by three-dimensional (3D) interchain charge transport.

B. Temperature dependence of the conductivity

The temperature dependence of the conductivity was measured by using both the colinear four-probe technique on samples cut parallel and perpendicular to the chain axis, and the Montgomery method on rectangular samples. Only the colinear four-probe data are shown, since the results obtained from both methods are similar. The value of ρ_r characterizes the quality of the samples; for all samples in the present work $\rho_r \approx 3$. The temperature dependence of conductivities are shown in Table I. Although $\sigma_\parallel \approx 10^5$ S/cm (parallel to the chain axis) has been reported, the positive temperature coefficient is not typical of that of a good metal, in which $\sigma(T)$ is limited by photon scattering.[1]

In previous studies, $\sigma(T)$ of highly conducting polyacetylene was analyzed in terms of the fluctuation induced tunneling (FIT) model.[19,20] However, a recent study has shown that this model is not satisfactory for highly conducting polyacetylene.[21] Although a $\log_{10}$ dependence of $\rho(T)$ was found to be satisfactory for samples having $\rho_r \approx 14$, the $\log_{10}T$ fit shows considerable deviation at low temperatures for samples having $\rho_r \approx 3-8$.[1] The plots of ρ versus $\log_{10}T$ and $\log_{10}\rho$ versus $\log_{10}T$ (for samples with $\rho_r \approx 3$) obtained in present study are shown in Fig. 3. In both cases the fit deviates below 20 K. Thus the dependences of ρ vs $\log_{10}T$ and $\log_{10}\rho$ vs $\log_{10}T$ are found to be satisfactory only in the case of $(CH)_x$ samples with intermediate disorder, and not for the best materials having $\rho_r < 4$.

In the critical regime of MIT in Anderson localization, the temperature dependence of resistivity follows a power law $[\rho(T) \propto T^{-\beta}]$.[22,23] The appropriate method to identify the critical regime is to plot, in a log-log scale, the reduced activation energy function $W(T)$ vs T, where $W = [-Td(\ln\rho)/dt]$.[24] In such a plot, the critical regime is easily identified from the temperature independence of W: $W_{\text{crit}} = \beta$. The $W(T)$ versus T plot for directions both parallel and perpendicular to the chain axis for samples with $\rho_r \approx 3$ is shown in Fig. 4. Although the anisotropy of conductivity is nearly 100 $W(T)$ is

TABLE I. Conductivity and the anisotropy of the conductivity at 250 and 1.2 K at ambient pressure and 8 kbar, for current parallel and perpendicular to the chain axis.

Current direction	Pressure (kbar)	250 K	1.2 K
		σ (S/cm)	σ (S/cm)
1. parallel to chain axis ($\sigma_\parallel$)	0	11 050	3670
2. perpendicular to chain axis ($\sigma_\perp$)	0	105	34.2
3. parallel to chain axis ($\sigma_\parallel$)	8	8460	3880
4. perpendicular to chain axis ($\sigma_\perp$)	8	127	45
		$\sigma_\parallel/\sigma_\perp$	$\sigma_\parallel/\sigma_\perp$
5. anisotropy of conductivity	0	105.2	107.3
6. anisotropy of conductivity	8	66.6	86.3

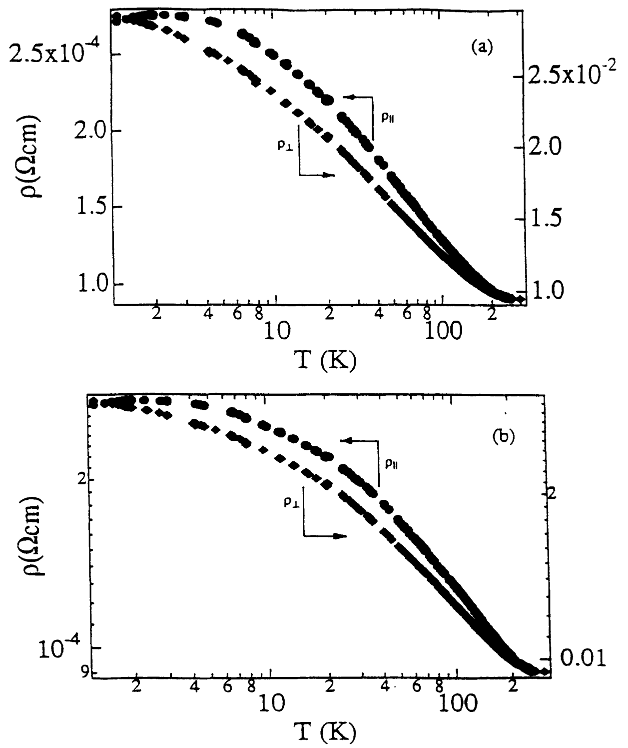

FIG. 3. (a) Resistivity vs log of temperature (T). (b) log-log plot of resistivity vs temperature for iodine-doped $(CH)_x$: (●) parallel to the chain axis, (◆) perpendicular to the chain axis.

identical in both directions. This indicates that the interfibrilar transport is sufficiently strong to produce identical temperature dependences for conductivity in directions both parallel and perpendicular to the chain axis. Moreover, for both directions, $W(T)$ is temperature independent from 180–60 K; below 60 K at ambient pressure, the positive temperature coefficient of $W(T)$ indicates that the transport is on the verge on the metallic side of the critical regime. Note that the conductivity parallel to the chain axis is much higher than Mott's minimum metallic value, as observed commonly in known systems near the MIT. However, the charge transport perpendicular to the chain axis is the limiting factor. Indeed, in the iodine-doped oriented polyacetylene samples, the conductivity perpendicular to the chain axis is of order 10^2 S/cm, i.e., close to the Mott value.

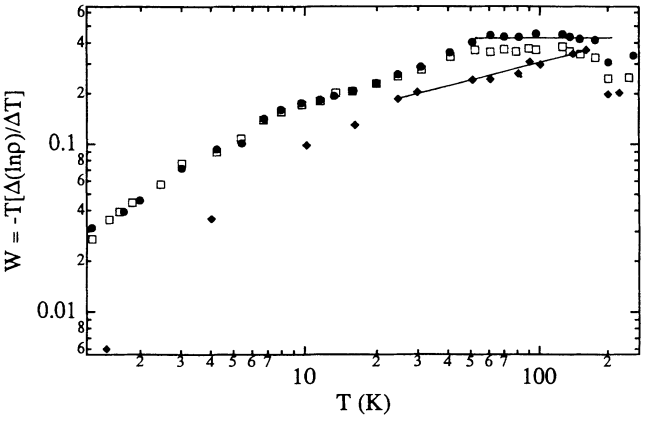

FIG. 4. Log-log plot of $W(T)$ vs temperature (T) for iodine-doped $(CH)_x$: (●) parallel to the chain axis, at ambient pressure; (□) perpendicular to the chain axis, at ambient pressure; and (◆) parallel to the chain axis at 8 kbar. The lines are drawn to guide the eye.

At high pressures, both ρ_r and the anisotropy of the conductivity have decreased due to the enhanced interchain transport. At 8 kbar, the system exhibits more metallic behavior due to the enhanced interchain transport, as shown in Fig. 4. When the value of ρ_r gradually increases above 3, the regime where $W(T)$ is temperature independent extends down to lower temperatures, whereas at high values of ρ_r ($\rho_r > 20$) the temperature dependence of $W(T)$ becomes negative.[25] Similar behavior has been observed in highly doped inorganic semiconductors[24] as well as in doped polyaniline[26] and polypyrrole.[27]

In the disordered metallic regime the conductivity at low temperatures is expressed by[2,3]

$$\sigma(T)=\sigma(0)+mT^{1/2}+BT^{p/2}, \tag{1}$$

where the second term ($T^{1/2}$) results from thermally induced electron diffusion through states near the Fermi energy (reduced by electron-electron scattering), and the third term is the correction to the zero-temperature conductivity due to localization effects. The value of p is determined by the temperature dependence of the scattering rate [$\tau^{-1} \propto T^p$] of the dominant dephasing mechanism. For electron-phonon scattering, $p=3$; for inelastic electron-electron scattering, $p=2$ and $\frac{3}{2}$ in the clean and

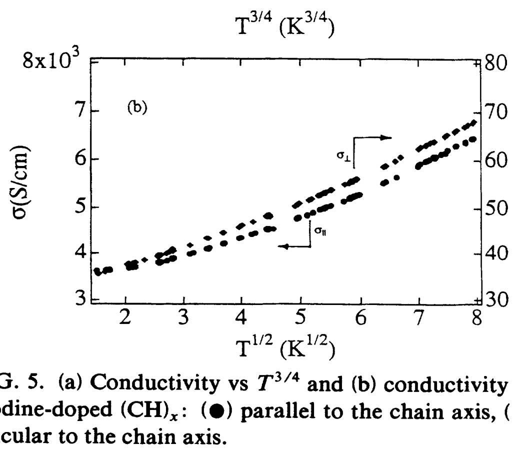

FIG. 5. (a) Conductivity vs $T^{3/4}$ and (b) conductivity vs $T^{1/2}$ for iodine-doped $(CH)_x$: (●) parallel to the chain axis, (◆) perpendicular to the chain axis.

dirty limits, respectively.[2,3]

Previous transport property measurements have shown that a three-dimensional localization-interaction model is valid for doped $(CH)_x$.[4,5,6] The $T^{1/2}$ and $T^{3/4}$ fits, for directions both parallel and perpendicular to the chain axis, are shown in Fig. 5. Although the anisotropy of conductivity is nearly 100, these fits are identical for directions both parallel and perpendicular to the chain axis. This indicates that the anisotropic three-dimensional model is appropriate for highly conducting $(CH)_x$. The linearity of the $T^{3/4}$ fits is better than that of the $T^{1/2}$ fits. This shows that the contribution from localization effects is dominant at temperatures above 3 K.[2,3] The $T^{3/4}$ fits indicates that the inelastic electron-electron scattering ($p=\frac{3}{2}$) in disordered metals is the dominant scattering mechanism. However, the $T^{1/2}$ fit at very low temperatures ($T<3$ K) indicates that electron-electron interactions are important. Thus localization and interaction effects dominate, respectively, at high and low temperatures. This has been confirmed through MC measurements, as described below.

The temperature dependence of conductivity at 8 kbar, both parallel and perpendicular to the chain axis, is shown in Fig. 6. Although the conductivity decreases above 4 kbar, the temperature dependence of conductivity at 8 kbar is substantially reduced under pressure. The values of ρ_r at ambient pressure and at 8 kbar, parallel (perpendicular) to the chain axis, are 3 (3) and 2.2 (2.8), respectively. This demonstrates that there is a substantial enhancement of the interchain transport under high pressure. Nevertheless, a positive temperature coefficient of the resistivity, typical for good metals, has not been observed. Thus even under high pressure the combination of interchain transport and disorder limit the mean free path.

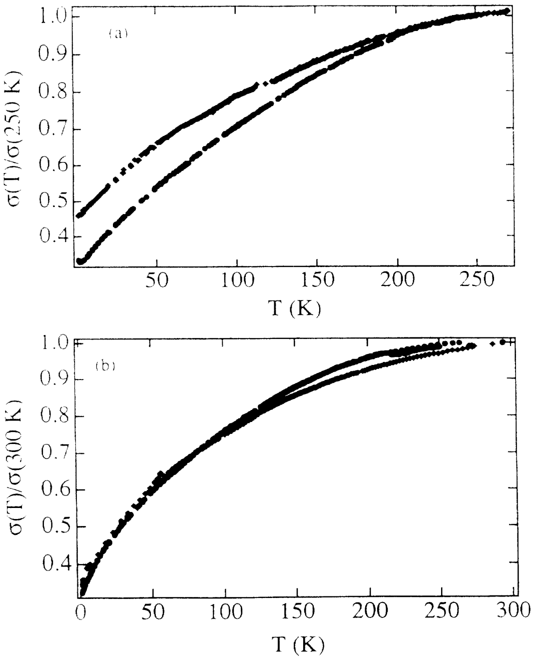

FIG. 6. Normalized conductivity $[\sigma(T)/\sigma(250\ \mathrm{K})]$ vs T for iodine-doped $(CH)_x$: (a) parallel to the chain axis; (b) perpendicular to the chain axis; (●) at ambient pressure; and (♦) at 8 kbar.

C. Magnetoconductance

Magnetoconductance measurements were carried out (by the collinear four-probe method) in all five different combinations of current direction with respect to the magnetic field and chain directions. Since the anisotropy (in conductivity) of the samples was approximately 100, anisotropic features could be observed in the MC. The anisotropic diffusion coefficient and the combination of effects from weak localization and electron-electron interaction yield a wide range of MC behavior.

In previous MC measurements of oriented $(CH)_x$ $[l/l_0\approx 5-10, \sigma_{\parallel}/\sigma_{\perp}\approx 25-50$, and the direction of the current parallel to the chain axis] a wide range of behavior including both positive and negative MC was observed.[5,6] The sign and magnitude of the MC was mainly determined by the extent of disorder, the direction of field with respect to the chain axis and temperature. When ρ_r decreases, the sign of the MC shifts from negative to positive.[5] For samples with intermediate disorder ($\rho_r\approx 3-6$), the sign of the MC was positive (negative) when the field was perpendicular (parallel) to the chain axis at temperatures above 2 K. Moreover, in both cases (whether the field is parallel or perpendicular to the chain axis) the magnitude of the positive MC decreased gradually as the temperature decreased from 10 to 2 K. The previous results clearly indicate that the weak-localization contribution (positive MC) dominates at higher temperatures, and that the contribution from electron-electron interactions (negative MC) dominates at lower temperatures.[5] When the extent of disorder is weaker ($\rho_r\leq 3$), the weak-localization contribution dom-

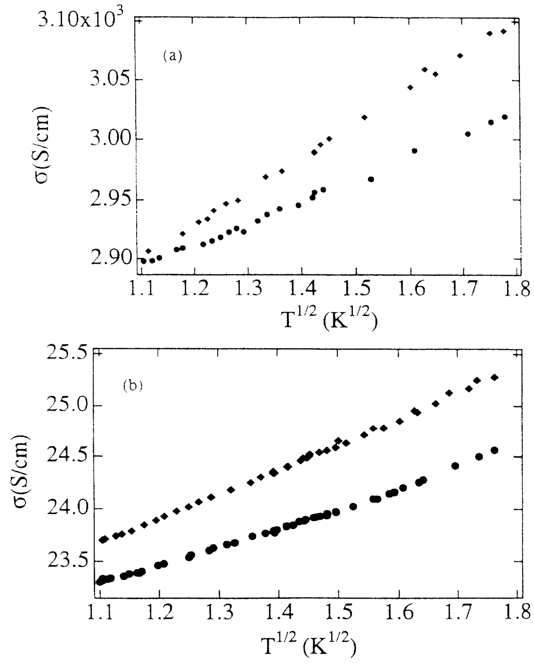

FIG. 7. Conductivity vs $T^{1/2}$ for iodine-doped $(CH)_x$: (a) parallel to the chain axis; (b) perpendicular to the chain axis; (●) at $H=0$; and (♦) at $H=8$ T.

TABLE II. The values of the parameters m^a, m (8 T), α, and γF_σ, and the temperature dependence of the inelastic scattering length for current parallel and perpendicular to the chain axis, and for the field perpendicular to the current and chain axis directions.

Field (H) vs current (I) vs chain axis (v)	m^a	m (8 T)	α	γF_σ	Inelastic scattering length (Å) 4.2 K	2 K	1.2 K
1. $H \perp v; I \parallel v; H \perp I$	195	316	283	0.43	644	902	1163
2. $H \perp v; L \perp v; H \perp I$	1.67	2.3	1.93	0.31	134	170	209

[a]In S cm^{-1} K$^{-1/2}$.

inates down to lower temperatures ($T \lesssim 1$ K), and the contribution from electron-electron interactions becomes important only at temperatures of the order of 1 K. Thus the anisotropy in both the conductivity and MC are related to the extent of misaligned chains in the samples and the anisotropy in the diffusion coefficient.[5]

The $T^{1/2}$ dependence of $\sigma(T)$ is shown in Fig. 7 for temperatures below 3 K. Although the temperature range of the $T^{1/2}$ fit is rather narrow, the interaction contribution at very low temperatures is clearly evident from the enhanced negative contribution to the MC. The existence of a $T^{1/2}$ term indicates that at very low temperatures, the contribution from electron-electron interactions in disordered metals plays the dominant role. Below 3 K, the temperature dependence of conductivity can be expressed as

$$\sigma(T)=\sigma(0)+mT^{1/2}\ , \tag{2a}$$

where

$$m=\alpha[(\tfrac{4}{3})-\gamma(3F_\sigma/2)]\ . \tag{2b}$$

α is a parameter depending on the diffusion coefficient, and γF_σ is the interaction parameter.[28,29] In a magnetic field,

$$\sigma(H,T)=\sigma(H,0)+m(H)T^{1/2}\ . \tag{3}$$

At fields sufficiently high that $g\mu_B H \gg k_B T$,

$$\sigma(H,T)=\sigma(H,0)+\alpha[(\tfrac{4}{3})-\gamma(F_\sigma/2)]T^{1/2}\ , \tag{4}$$

assuming that α, γ, and F_σ are not dependent on the magnetic field.[29]

The parameters α and γF_σ can be estimated from the values of m and $m(H)$ obtained at $H=0$ and 8 T, respectively, by using Eqs. (2) and (4). Note that for $T<8$ K, $g\mu_B H > k_B T$. The values of m, $m(H)$, α, and γF_σ are summarized in Table II. The extrapolated values of $\sigma(0)$ to $T=0$ are

$$\sigma_\parallel(0)\approx 3600\ \text{S/cm}\ ,$$

$$\sigma_\perp(0)\approx 30\ \text{S/cm at ambient pressure}\ ,$$

$$\sigma_\parallel(0)\approx 3800\ \text{S/cm},\quad \sigma_\perp(0)\approx 40\ \text{S/cm at 8 kbar}\ .$$

Although the value of $\sigma_\parallel(0)$ exceeds the one typical of systems near MIT, values of $\sigma(0)$ as large as 4135 S/cm have been reported for $Y_x\text{Si}_{1-x}$.[30] However, it is well known that $\sigma(0)$ in disordered metals is sensitive to the extent of the disorder and resistivity ratio. Since the conductivity parallel to the chain axis (of the order of 10^3 S/cm) exceeds that typical of systems near the M-I transition, the values of m and α are unusually large. However, the values of m, α and conductivity in the direction perpendicular to the chain axis are typical of systems near the M-I transition. Thus the localization-interaction model near the M-I transition is appropriate for the analysis of MC data in the direction perpendicular to the chain axis.

The MC for current parallel to the chain axis is shown in Fig. 8. When the field (current) is perpendicular (parallel) to the chain direction, the MC is positive; however, the magnitude of positive contribution starts decreasing at 1.2 K, as shown in Fig. 8(a). This is due to the interplay of weak-localization and electron-electron-interaction contributions. Nevertheless, when the field (current) is parallel (parallel) to the chain direction the sign of the MC is always negative, and its magnitude increases at low temperatures, as shown in Fig. 8(b). This

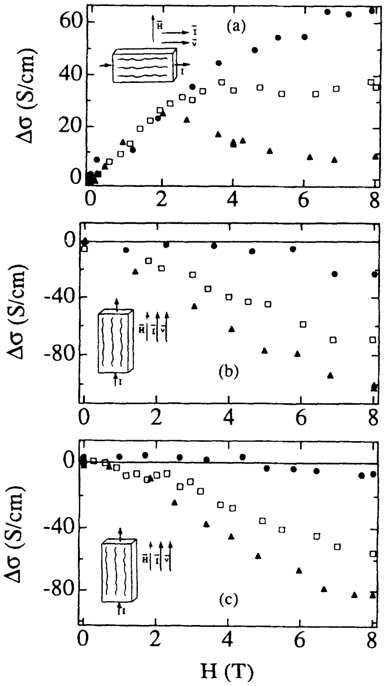

FIG. 8. Magnetoconductance $[\sigma(H,T)-\sigma(0,T)]$ vs magnetic field for iodine-doped $(\text{CH})_x$ at 4.2 K (●), 2 K (□), and 1.2 K (▲). The current is parallel to chain axis (v): (a) field is perpendicular (perpendicular) to the chain axis (current); (b) field is parallel (parallel) to the chain axis (current) at ambient pressure; and (c) field is parallel (parallel) to the chain axis (current) at 8 kbar.

anisotropy in the MC is attributed to the anisotropic diffusion coefficient. This is proven by the MC measurements under high pressure. At 4.2 K, the anisotropy in conductivity at ambient pressure and 8 kbar are 98 and 77, respectively. The enhancement of interchain interaction at high pressures reduces the anisotropy in both the conductivity and diffusion coefficient. The MC at 8 kbar with the field (current) parallel (parallel) to the chain axis is shown in Fig. 8(c). For fields below 4 T, the sign of the MC has reversed from negative to positive at 4.2 K (8 kbar); and at higher fields, the sign remains negative due to the dominant contribution from electron-electron interactions, as shown in Fig. 8(c). Moreover, the magnitude of the negative MC at temperatures below 4.2 K is reduced under pressure. This shows that the sign and magnitude of the MC in oriented $(CH)_x$ depend on the anisotropic diffusion coefficient.[31]

The MC for current direction perpendicular to the chain axis is shown in Fig. 9. At 4.2 K, the MC is positive when the field (current) is perpendicular (perpendicular) to the chain direction [shown in Figs. 9(a) and 9(b)]. This is due to the dominant contribution from weak localization at 4.2 K. Since the contribution from electron-electron interaction increases at lower temperatures and higher magnetic fields, the sign of the MC has reversed from positive to negative at 1.2 K and $H\approx 4$ T. The MC in the case of current (field) perpendicular (parallel) to the chain axis is shown in Fig. 9(c). The sign of MC is negative, similar to the case when the current (field) is parallel (parallel) to the chain direction, as shown in Fig. 8(b). This shows that the anisotropic MC is not caused by the direction of current with respect to chain axis. The anisotropic MC is due to the anisotropic diffusion coefficient, which in turn is a function of the angle between the field direction and chain axis.[31]

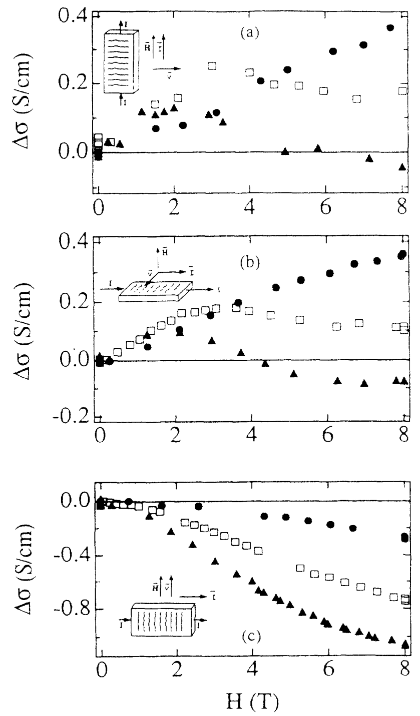

FIG. 9. Magnetoconductance $[\sigma(H,T)\text{-}\sigma(0,T)]$ vs magnetic field for iodine-doped $(CH)_x$ at 4.2 K (●), 2 K (□), and 1.2 K (▲). The current is perpendicular to the chain axis (v): (a) field is perpendicular (parallel) to the chain axis (current); (b) field is perpendicular (perpendicular) to the chain axis (current); and (c) field is parallel (perpendicular) to the chain axis (current).

Apparently, in samples having $\rho_r\approx 3-5$, similar anisotropy in the MC has been observed previously (between 4.2 and 1.6 K).[5] Although the sign of the MC did not change for samples having $\rho_r\leq 3$, the magnitude of the positive MC is nearly three times larger when the field is perpendicular to the chain as compared to the case when the field is parallel to the chain direction.[5] This clearly indicates that the interaction contribution to the MC is larger in the latter case due to the anisotropic diffusion coefficient. Moreover, the field-induced crossover from positive to negative MC shown in Figs. 9(a) and 9(b) indicates the interplay between the contributions to the MC from weak localization and electron-electron interaction.

The contribution to $\Delta\Sigma(H,T)=\sigma(H,T)-\sigma(0,T)$ from electron-electron interactions can be written as follows:[28,29]

$$\Delta\Sigma_I(H,T)=-0.041(g\mu_B/k_B)^2\gamma F_\sigma T^{-3/2}H^2 \qquad (g\mu_B H \ll k_B T)\ , \tag{5a}$$

$$\Delta\Sigma_I(H,T)=\alpha\gamma F_\sigma T^{1/2}-0.77\alpha(g\mu_B/k_B)^{1/2}\gamma F_\sigma H^{1/2} \qquad (g\mu_B H \gg k_B T)\ . \tag{5b}$$

At low and high fields, $\Delta\Sigma_I(H,T)$ is proportional to H^2 and $H^{1/2}$, respectively.

For the low-magnetic-field regime, we follow Rosenbaum *et al.*[28] and assume that the contributions to $\Delta\Sigma(H,T)$ which arise from electron-electron interaction and weak localizations are additive. Thus the total low-field MC is given by

$$\Delta\Sigma(H,T)=-0.041\alpha(g\mu_B/k_B)^2\gamma F_\sigma T^{-3/2}H^2 +(1/12\pi^2)(e/c\hbar)^2G_0(l_{\text{in}})^3H^2\ , \tag{6}$$

where $G_0=(e^2/\hbar)$, and l_{in} is the inelastic scattering length. The first term on the right-hand side is the contribution from electron-electron interactions (negative MC), and the second term on the right-hand side is the contribution from weak localization (positive MC). The first term can be estimated by using values for α and γF_σ obtained above. Then, using the slope of $\Delta\Sigma(H,T)$ vs H^2, in the low-field region, the second term can be estimated. In this way the value of the inelastic scattering length can be calculated at each temperature. The values of inelastic scattering length at different temperatures, for directions both parallel and perpendicular to the chain axis, are shown in Table II. At 1.2 K, the inelastic scattering lengths in directions parallel and perpendicular to the chain axis are 1163 and 210 Å, respectively. The temperature dependence of the inelastic scattering length is shown in Fig. 10. The $T^{-3/4}$ dependence of the inelastic scattering length, in directions both parallel and perpendicular to the chain axis, is typical to that of inelastic

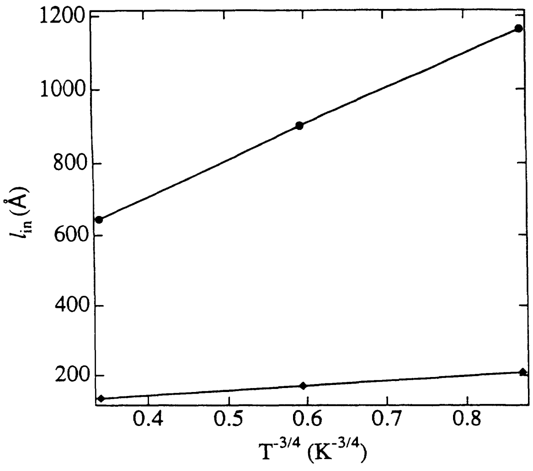

FIG. 10. The inelastic scattering length vs $T^{-3/4}$ for iodine-doped $(CH)_x$: (●) parallel and (◆) perpendicular to the chain's axis.

electron-electron scattering in disordered metals.[2,3] This is in agreement with the $T^{3/4}$ dependence of the conductivity, as shown earlier in Fig. 5(a). Thus both the conductivity and MC are consistent with the localization-interaction model of anisotropic disordered metals.

IV. CONCLUSION

A comprehensive study of the conductivity and MC has been carried out for directions both parallel and perpendicular to the chain axis, as a function of pressure, temperature, and magnetic field. The room-temperature conductivity increases up to 4 kbar, and at higher pressure the conductivity gradually decreases. At 8 kbar, the temperature dependence of the conductivity ($\sigma_{\parallel}$) and the anisotropy in the conductivity ($\sigma_{\parallel}/\sigma_{\perp}$) have decreased by factors of 1.4 and 1.6, respectively. $W(T)$ is temperature independent from 180 to 60 K in directions both parallel and perpendicular to the chain axis. This indicates that at ambient pressure the system is on the verge of the metallic side of the critical regime. However, at 8 kbar, the system exhibits more metallic behavior due to the enhanced interchain transport. The $T^{3/4}$ dependence of the conductivity above 3 K indicates that inelastic electron-electron scattering in disordered metals is the dominant scattering process. However, at temperatures below 3 K, the $T^{1/2}$ dependence of the conductivity arises from the residual electron-electron interaction.

The sign and magnitude of the MC is determined by the extent of the disorder, the temperature, the degree of orientation of the chains in the sample, and the angle between the magnetic field and the chain axis. In samples with high anisotropy ($\sigma_{\parallel}/\sigma_{\perp} \geq 100$) and less disorder ($\rho_r \leq 3$), the sign of the MC is positive (negative) when the field is perpendicular (parallel) to the chain axis. Whether the field is parallel or perpendicular to the chain axis, the electron-electron-interaction contribution (negative MC) dominates over the weak-localization contribution (positive MC) at high fields and low temperatures. The anisotropic MC is due mainly to the anisotropic diffusion coefficient, as confirmed by the crossover from negative to positive MC and the reduced magnitude of the negative MC at 8 kbar. At 1.2 K, the inelastic scattering length for directions parallel and perpendicular to the chain axis are 1163 and 210 Å, respectively. The $T^{-3/4}$ dependence of the inelastic scattering length is consistent with the $T^{3/4}$ dependence of the conductivity at low temperatures, indicating that the inelastic electron-electron scattering in disordered metals is the dominant scattering mechanism.

ACKNOWLEDGMENTS

We express our gratitude to A. J. Heeger for important discussions. This work was partially supported by the MRL Program of the National Science Foundation under Award No. DMR-9123048. We thank M. Andersson for assistance in the earlier stages of this work, and Dr. C. O. Yoon for discussions. K. V. was supported by a grant from Neste Oy, Finland.

---

*Present address: Corporate R&D, Neste OY, P.O. Box 310, SF-06101 Porvoo, Finland.

†Present address: UNIAX Corporation, 5375 Overpass Rd., Santa Barbara, CA 93111.

[1] T. Ishiguro, H. Kaneko, Y. Nogami, H. Ishimoto, N. Nishiyama, J. Tsukamoto, A. Takahashi, M. Yamamura, T. Hagiwara, and K. Sato, Phys. Rev. Lett. **69**, 660 (1992).

[2] *Electron-Electron Interaction in Disordered Conductors,* edited by A. L. Efros and M. Pollak (North-Holland, Amsterdam, 1985).

[3] P. A. Lee and T. V. Ramakrishnan, Rev. Mod. Phys. **57**, 287 (1985).

[4] G. Thummes, U. Zimmer, F. Korner, and J. Kotzler, Jpn. J. Appl. Phys. Suppl. **26-3**, 713 (1987); G. Thummes, E. Korner, and J. Kotzler, Solid State Commun. **67**, 215 (1988).

[5] Y. Nogami, H. Kaneko, H. Ito, T. Ishiguro, T. Sasaki, N. Toyota, A. Takahashi, and J. Tsukamoto, Phys. Rev. B **43**, 11 829 (1991).

[6] H. H. S. Javadi, A. Chakraborty, C. Li, N. Theophilou, D. B. Swanson, A. G. MacDiarmid, and A. J. Epstein, Phys. Rev. B **43**, 2183 (1991).

[7] M. J. Winokur, J. Maron, Yong Cao, and A. J. Heeger, Phys. Rev. B **45**, 9656 (1992).

[8] Y. Wada, in *Physics and Chemistry of Materials with Low-Dimensional Structures,* edited by H. Aoki, M. Tsukada, M. Schluter, and F. Levy (Kluwer Academic, Dordrecht, 1992).

[9] A. Kawabata, Solid State Commun. **34**, 431 (1980); J. Phys. Soc. Jpn. **49**, 628 (1980).

[10] B. L. Al'tshuler, A. G. Aronov, A. I. Larkin, and D. E. Khmel'nitskii, Zh. Eksp. Teor. Fiz. **81**, 768 (1981) [Sov. Phys. JETP **54**, 411 (1981)].

[11] K. Akagi, M. Suezaki, H. Shirakawa, H. Kyotani, M. Shimomura, and T. Tanabe, Synth. Met. **28**, D1 (1989).

[12] Yong Cao, Paul Smith, and A. J. Heeger, Polymer **32**, 545 (1991).

[13] H. C. Montgomery, J. Appl. Phys. **42**, 2971 (1971).

[14] A. Jayaraman, A. R. Huston, J. H. McFee, A. S. Coriell, and R. C. Maines, Rev. Sci. Instrum. **38**, 44 (1967).

[15] H. Fujiwara, H. Kadomatsu, and K. Tohma, Rev. Sci. Instrum. **51**, 1345 (1980).

[16] D. Moses, J. Chen, A. Denenstein, M. Kaveh, T.-C. Chung, A. J. Heeger, A. G. MacDiarmid, and Y. W. Park, Solid State Commun. **40**, 1007 (1981).

[17] N. Basescu, J. Chiang, S. Rughooputh, T. Kubo, C. Fite, and A. J. Heeger, Synth. Met. **28**, D43 (1989).

[18] K. Väkiparta, M. Reghu, M. R. Andersson, Y. Cao, D. Moses, and A. J. Heeger, Phys. Rev. B **47**, 9977 (1993); M. R. Andersson, K. Väkiparta, M. Reghu, Y. Cao, and D. Moses, *ibid.* **47**, 9238 (1993).

[19] P. Sheng, Phys. Rev. B **21**, 2180 (1980).

[20] A. B. Kaiser, Synth. Met. **45**, 183 (1991).

[21] Y. Nogami, M. Yamashita, H. Kaneko, T. Ishiguro, A. Takahashi, and J. Tsukamoto, J. Phys. Soc. Jpn. **62**, 664 (1993).

[22] W. L. C. McMillan, Phys. Rev. B **24**, 2739 (1981).

[23] A. I. Larkin and D. E. Khmelnitskii, Zh. Eksp. Teor. Fiz. **83**, 1140 (1982) [Sov. Phys. JETP **56**, 647 (1982)].

[24] A. G. Zabrodskii and K. N. Zeninova, Zh. Eksp. Teor. Fiz. **86**, 727 (1984) [Sov. Phys. JETP **59**, 425 (1984)].

[25] M. Reghu, K. Vakiparta, C. O. Yoon, Y. Cao, D. Moses, and A. J. Heeger, Synth. Met. (to be published).

[26] M. Reghu, Y. Cao, D. Moses, and A. J. Heeger, Phys. Rev. B **47**, 1758 (1993); M. Reghu, C. O. Yoon, Y. Cao, D. Moses, and A. H. Heeger, *ibid.* **48**, 17 685 (1993).

[27] C. O. Yoon, M. Reghu, D. Moses, and A. J. Heeger, Phys. Rev. B **49**, 10 851 (1994).

[28] T. F. Rosenbaum, R. M. F. Milligan, G. A. Thomas, P. A. Lee, T. V. Tamakrishnan, and R. N. Bhatt, Phys. Rev. Lett. **47**, 1758 (1981).

[29] Peihua Dai, Youchu Zhang, and M. P. Sarachik, Phys. Rev. B **45**, 3984 (1992); **46**, 6724 (1992).

[30] P. Hernandez and M. Sanquer, Phys. Rev. Lett. **68**, 1402 (1992).

[31] V. N. Prigodin and S. Roth, Synth. Met. **53**, 237 (1993).